ResearchGate

See discussions, stats, and author profiles for this publication at: https://www.researchgate.net/publication/242525735

FLOOD INUNDATION MAP OF BANGLADESH USING MODIS SURFACE REFLECTANCE DATA

Article · January 2009

CITATIONS
16

READS
3,292

3 authors, including:

Sujit Kumar Bala
Bangladesh University of Engineering and Technology
33 PUBLICATIONS **872** CITATIONS

SEE PROFILE

Anisul Haque
Bangladesh University of Engineering and Technology
100 PUBLICATIONS **674** CITATIONS

SEE PROFILE

Some of the authors of this publication are also working on these related projects:

DEltas, vulnerability and Climate Change: Migration and Adaptation (DECCMA) View project

Deltas, Vulnerability & Climate Change: Migration & Adaptation View project

All content following this page was uploaded by Sujit Kumar Bala on 29 May 2014.

The user has requested enhancement of the downloaded file.

Journal of
Flood Risk Management

Flood inundation map of Bangladesh using MODIS time-series images

A.S. Islam, S.K. Bala and M.A. Haque

Institute of Water and Flood Management, Bangladesh University of Engineering and Technology, Dhaka, Bangladesh

Correspondence:
Akm Saiful Islam, Institute of Water and Flood Management, Bangladesh University of Engineering and Technology, Dhaka 1000, Bangladesh
Tel: +88 01 716 449 657
Fax: +88 02 861 3046
Email: akmsaifulislam@iwfm.buet.ac.bd

DOI:10.1111/j.1753-318X.2010.01074.x

Key words
EVI; LSWI; NDVI; MODIS; RADARSAT.

Abstract

The detection of the spatio-temporal extent of inundation resulting from the floods in 2004 and 2007 in Bangladesh has been studied using time-series MODIS surface reflectance data. Flood inundation maps were developed from vegetation and land water surface indices derived using surface reflectance. The inundation map developed using MODIS data was compared with a corresponding RADARSAT image, where both images refer to the satellite-based remote-sensing data. The estimates show a strong correlation with the inundation area derived from the RADARSAT products (coefficient of determination of R^2: 0.96). The paper shows that it is possible to study flood dynamics by assessing inundation and recession patterns and to perform flood assessments similar to the high-resolution (50 m) microwave satellite, RADARSAT-based flood assessments using products derived from MODIS 500 m imagery. MODIS has advantages over microwave satellite because it has a high observational frequency and these data are available free of cost. We have concluded that this is a useful method to assess the extent of the temporal floods in the People's Republic of Bangladesh.

Introduction

Flooding is a very common phenomenon in the People's Republic of Bangladesh. The geographic location of the country is such that natural river floods occur almost every year during the monsoon season between June and September. Every year, one-quarter to one-third of the country is inundated by overflowing rivers during the monsoon season. The floods disrupt the lives of people. In the urban areas, floods damage property, infrastructure and road networks while floods in rural areas frequently also cause damage to crops and loss of livestock. Floods place people's live at risk both directly through drowning and also by disrupting communications. On the other hand, floods have a positive impact on the environment. For example, floodwaters supply nutrients that enrich the soil and recharge groundwater. Although solid wastes are washed out, floods enhance the diversity of aquatic species. Severe floods even have a positive effect on rice production in Bangladesh (Asada *et al.*, 2005). Many studies have been carried out to investigate the hydrologic behaviour of the floods in Bangladesh (Chowdhury *et al.*, 1998; Islam and Chowdhury, 2002; Rahman *et al.*, 2005; Islam, 2006). However, research on the determination of the real-time mapping of the flood inundation in Bangladesh has been limited in comparison with the wide range of research conducted in other countries. The temporal and spatial extent of flood inundation is important for the evaluation of the relationships between the water regime and local agricultural activity and the behaviour of the global ecosystem. Floods not only affect human beings but also affect various components of the ecosystem concerned. Therefore, the start date and the duration of floods play a vital role in the economy of the country.

Remote-sensing images can be an effective and efficient tool for the determination of flood inundation areas and this is the focus of this paper. Many studies have been conducted using remote-sensing data to detect spatial and temporal changes in the extent of the flood inundation, including the delineation of wetlands, and also to study the changes (Martineza *et al.*, 2007; Sahoo *et al.*, 2006; Hossain *et al.*, 2007). These have made it possible to assess flood damage in urban areas, as well as the dynamics and behaviour of floods. These studies mainly detect the extent of surface water using a range of sensors attached to satellites. The selection of suitable sensors that are both cost effective and efficient in the development of the flood inundation map is a major challenge. One major problem

© The Authors
Journal of Flood Risk Management © 2010 CIWEM and Blackwell Publishing Ltd

with optical sensors is their inability to penetrate clouds. The land surface is obscured with clouds on most days when flooding occurs in the monsoon period. Under these circumstances, the synthetic aperture radar (SAR) has been considered the most effective sensor in detecting flood inundation areas. In the past, the images taken from various satellites such as RADARSAT, JERS-1, ERS-1/2 and ENVISAT have also been used to detect inundated areas in a number of ways for example, through the rule-based analysis of polarized data (Hirose *et al*., 2001; Henry *et al*., 2003), object-oriented classification (Heremans *et al*., 2005), filtering of microware data (Ishitsuka *et al*., 2003), high temporal detection (Laugier *et al*., 1997), rule-based analysis of SAR data (Nguyen and Bui, 2001; Wang, 2002, 2004) and combining both SAR and RADARSAT images (Liew *et al*., 1998).

Although RADARSAT and other SARs are capable of monitoring land surfaces, it is not feasible to use them for monitoring large areas for a long time. The costs involved in obtaining these data are high, for example, RADARSAT images per scene are currently approximately US$3600 per scene. The coverage area varies with the resolution of the scene. For example, a fine RADARSAT image of resolution of 8 m has a coverage area of 50 km × 50 km. Alternatively, a ScanSAR narrow RADARSAT image of resolution of 50 m has a coverage area of 300 km × 300 km. To minimize the cost of production, inundation maps have also been developed using data from various low-resolution optical sensors. The following alternative means of mapping the surface water: (i) data from NOAA/AVHRR of 1.1 km, (ii) SPOT of 1 km (Harris and Mason, 1989; Liu *et al*., 2002; Xiao *et al*., 2002a), (iii) SSM/I of 13 km and (iv) MOS/SMR of 23 km spatial resolution (Jin, 1999; Tanaka *et al*., 2000, 2003) have been considered as an alternative means of mapping the extent of surface water. Most of these data are freely available from the Internet on a daily basis, which makes it possible to detect changes in the inundation of areas that may be large.

The spatial resolutions of SSM/I and MOS/SMR are very low in comparison with NOAA/AVHRR and SPOT data. This makes NOAA/AVHRR and SPOT more effective tools for detecting inundation and temporal changes in the extent of the flooded areas. Various techniques such as the discrimination of low cloud coverage by Bryant and Rainey (2002) and discrimination between water and land surfaces using band ratios (Sheng and Gong (2001) have also been developed to reduce and detect the effects of cloud cover. Deriving indices, such as the normalized difference water index (NDWI) by Xiao *et al*. (2002b), are also efficient in detecting inundation and the transplantation of rice crops.

In December 1999, immediately after its launch, the MODIS satellite's moderate-resolution optical sensor of 250–500 m became a useful tool for scientific research. Many studies have been conducted to determine the extent of surface water where vegetation growth occurs, for example, to estimate its extent in paddy fields by Xiao *et al*. (2005, 2006) and the detection of inundation areas through vegetation cover conversion by Zhan *et al*. (2002). The Dartmouth Flood Observatory (2006) also uses MODIS data to monitor flood disasters all over the world. The observatory published an annual inundation map of Bangladesh via the Internet (Anderson *et al*., 2005) until 2007.

Sakamoto *et al*. (2007) have developed a methodology to detect spatio-temporal flood distributions in Cambodia and Vietnam using MODIS data. The main advantages of this methodology are: (1) time-series data are available during flood periods; (2) global data are available; (3) the data can be downloaded free of charge through the Internet; and (4) the accuracy of the flood inundation map lies within the acceptable range. However, the application of their methodology to flood inundation mapping in Bangladesh is a difficult task, due to the dissimilarity of the hydro-geological conditions in Cambodia, Vietnam and Bangladesh. Some modifications are essential to adopt the methodology for different situation as proposed in this study. Using this modified methodology, spatio-temporal changes in the extent of the flood inundation have been studied in Bangladesh. The temporal changes in the extent of inundation in Bangladesh were assessed at a resolution of 500 m for major floods in 2004 and 2007.

Study area

Bangladesh is located between latitude 20–27°N and longitude 88–93°E (Figure 1). The country lies in the floodplain delta of three major river basins: the Ganges; the Brahmaputra; and the Meghna (GBM). About 80% of the annual rainfall of Bangladesh occurs during the monsoon season between June and September. The major cause of the monsoon flood stems from the intensity, duration and magnitude of the rainfall in the GBM basin. Every year, one-quarter to one-third of the country is inundated during the monsoon season by overflowing rivers. However, the degree of this inundation sometimes becomes severe, causing damage to infrastructures, crops, communication systems and risking the lives of people. The floods in 2004 and 2007 were severe in both their magnitude and duration and were observed to have a huge impact on the society of the area and on nature.

Spectral signatures are a specific combination of reflected and absorbed electromagnetic radiation at varying wavelengths that can uniquely identify an object. The spectral signatures using various bands of MODIS images are unique for different land-use types. It is very important to properly classify the different spectral signatures within the satellite imaging associated with different types of land use and inundation. A total of nine categories of land use/land type

© The Authors
Journal of Flood Risk Management © 2010 CIWEM and Blackwell Publishing Ltd

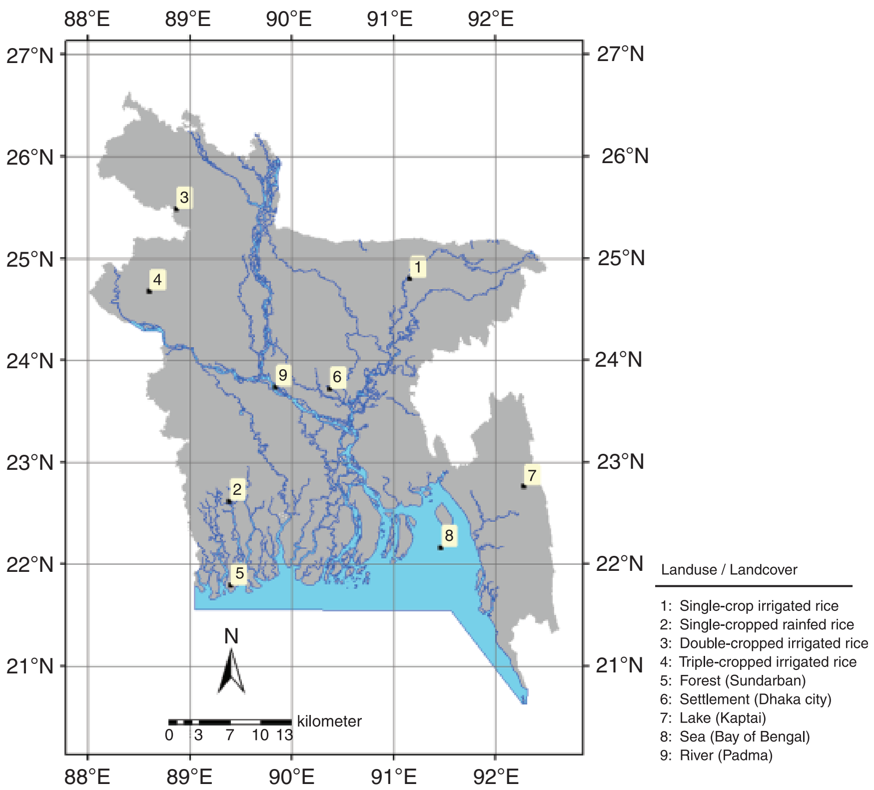

Figure 1 Location map of the study area.

have been selected to analyse the inundation areas (Figure 1). These are (1) single-crop rain fed rice in the Haor area of northeastern region of Bangladesh; (2) single-crop irrigated rice in the southwestern region; (3) double-cropped irrigated rice in the northern region; (4) triple-cropped irrigated rice in the Brand area of the northwestern region; (5) forest area of the Sundarbans; (6) settlement area of Dhaka city; (7) Kaptai Lake; (8) Bay of Bengal Ocean; and (9) Padma River. The temporal variations of various indices based on spectral reflections sensed by satellite on those nine land-use categories will be discussed in the following subsection.

Data

MODIS/TERRA time-series data

This study uses MODIS satellite images acquired by the TERRA instrument, which can be freely downloaded through the Earth Observing System Data Gateway (EOS, 2006). This study analysed 8-day composite data from MODIS, taken during 2007 and 2004. The full title of this product is 'MODIS/TERRA SURFACE REFLECTANCE 8-DAY L3 GLOBAL 500 M SIN GRID V005'. The spatial resolution of these images is approximately 500 m. Correction of the images to remove the effects of atmosphere has already been carried out (Vermote and Vermeulen, 1999). These data are taken every 8 days and are delivered as a composite product called MOD09, which took the best surface spectral reflectance in this period with the least effect of aerosols and other atmospheric ingredients.

Flood inundation map based on RADARSAT images

The inundation maps produced by the Center for Environmental Geographic Information Services are used as a reference to evaluate the estimates derived from MODIS data. The map is based on the Digital Elevation Model (DEM) data, hydrological data and RADARSAT images, and was acquired on the 3 August 2007 or, day of the year (DOY) of 215, using the ScanSAR Narrow B Mode. As C-band microwaves can penetrate cloud cover and easily discriminate open water on the basis of backscatter coefficient data at a high resolution (50 m), it has been assumed that the inundation map based on the RADARSAT images reveals the details of flood distribution at a satisfactory spatial resolution, even under cloud coverage. The inundated areas in this map were aggregated within each grid at 500 m resolution to enable comparisons with the results derived from the MODIS data.

© The Authors
Journal of Flood Risk Management © 2010 CIWEM and Blackwell Publishing Ltd

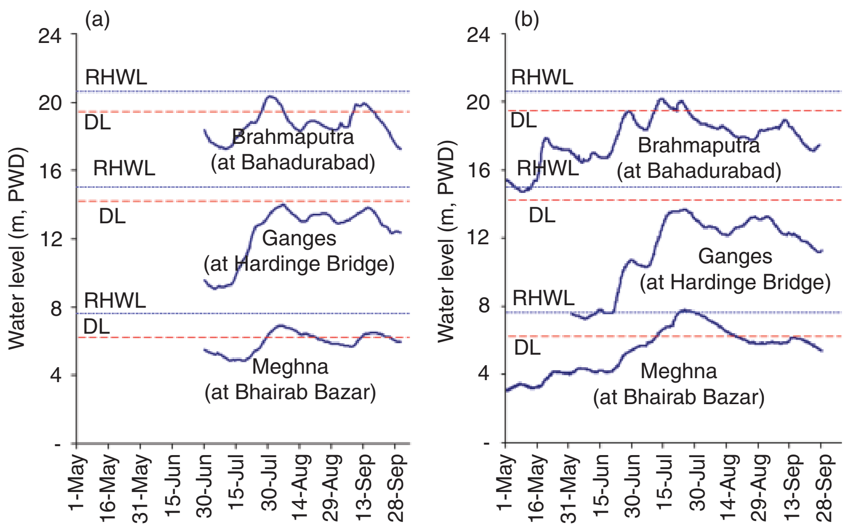

Figure 2 Water-level hydrographs of major rivers in Bangladesh for (a) Year 2007 and (b) Year 2004. Flood started earlier in 2004 than in 2007.

Table 1 Hydrologic characteristic of floods in Bangladesh

Parameters	River	Gauge station	2007	2004
Height of peak flood level in metres above the danger level	Brahmaputra	Bahadurabad	0.88	0.68
	Ganges	Hardinge Bridge	–	–
	Meghna	Bhairab Bazaar	0.69	1.53
Duration of flood in days above the danger level	Brahmaputra	Bahadurabad	21	15
	Ganges	Hardinge Bridge	0	0
	Meghna	Bhairab Bazaar	37	38

Water-level data for major rivers in Bangladesh

The three major rivers of the country – GBM, carry the huge amount of water that results from rainfall within their catchments. During the rainy season, a flood occurs when the water level crosses a certain predefined level known as the danger level (DL). For each river, the DL and the previous recorded high water level are established by the national Flood Forecasting and Warning Center before the start of the rainy season. Figure 2 shows the time series of the daily-averaged water-level hydrographs for the major rivers in Bangladesh for 2007 and 2004. Water-level data from one gauging station in each major river are used for this comparison. The three locations were the Bahadurabad station of the Brahmaputra; the Hardinge Bridge station of the Ganges; and the Bhariab Bazar station of the Meghna. These are very well-known gauging stations with good records of historic floods. The magnitude of the peak floods and duration of days above the DL in the GBM have been presented in Table 1.

Methods

Detecting water-related surface using MODIS data

In the past, the normalized difference vegetation index (NDVI) and the NDWI have been used to identify surface waters (Rogers and Kearney, 2004). The main reason for using NDWI is that short-wave infrared (SWIR) is highly sensitive to the moisture content in the soil and the vegetation canopy. A number of studies have been conducted utilizing the spectroscopic characterization of SWIR to detect water content (Gao, 1996; McFeeters, 1996; Jackson *et al.*, 2004; Rogers and Kearney, 2004; Tong *et al.*, 2004). Xiao *et al.* (2002b) showed that NDWI in paddy fields exceeds NDVI derived from SPOT data for the same period of flooding and rice planting in eastern Jiangsu Province, China. In recent years, Xiao *et al.* (2005, 2006) used anomalies between the land surface water index (LSWI) and the vegetation indexes (NDVI or EVI; see Table 2) in an algorithm to estimate the distribution of paddy fields in southern China and South and Southeast Asia. The detailed description of the indices derived from MODIS data is presented in Table 2, along with the band number and solar spectrum.

The enhanced vegetation index is an optimization of NDVI by implementing a set of coefficients in the NDVI equation. This addition improves the result found purely by the vegetation signal. A soil background correction and an atmosphere resistance term have been introduced to calculate EVI. The main purpose of the optimization used in EVI is to isolate the photosynthetically active signal from the

© The Authors
Journal of Flood Risk Management © 2010 CIWEM and Blackwell Publishing Ltd

Table 2 Definition of MODIS-derived indices used to detect the spatial and temporal distribution of flood

Indices	Equation
Normalized difference vegetation index (NDVI)	$\mathrm{NDVI} = \frac{\rho_{NIR} - \rho_{Red}}{\rho_{NIR} + \rho_{Red}}$
Normalized difference water index (NDWI)	$\mathrm{NDWI} = \frac{\rho_{Red} - \rho_{SWIR}}{\rho_{Red} + \rho_{SWIR}}$
Enhanced vegetation index (EVI)	$\mathrm{EVI} = 2.5 \times \frac{\rho_{NIR} - \rho_{Red}}{\rho_{NIR} + 6 \times \rho_{Red} - 7.5 \times \rho_{Blue} + 1}$
Land surface water index (LSWI)	$\mathrm{LSWI} = \frac{\rho_{NIR} - \rho_{SWIR}}{\rho_{NIR} + \rho_{SWIR}}$

ρ_{NIR} is the reflectance of near infrared (841–875 nm, MODIS band 2), ρ_{Red} is the reflectance of red (621–670 nm, MODIS band 1), ρ_{Blue} is the reflectance of blue (459–479 nm, MODIS band 3) and ρ_{NIR} is the reflectance of short-wave infrared (1628–1652 nm, MODIS band 6) of the solar spectrum. The parameters adopted in the MODIS-EVI algorithm are $L = 1$, $C1 = 6$, $C2 = 7.5$ and G (gain factor) = 2.5.

mixed or contaminated pixels. The parameters used in the EVI equation are L as the canopy background adjustment that addresses nonlinear, differential NIR and red radiant transfer through a canopy, and C1, C2 are the coefficients of the aerosol resistance term, which uses the blue band to correct for aerosol influences in the red band. The parameters adopted in this study are from the MODIS-EVI algorithm (TBRS, 2002). However, a further study to find optimum values of these parameters to calculate EVI for this region can be carried out, which is beyond the scope of this paper.

The methodology used in this study is a modified approach based on the technique originally developed by Sakamoto *et al.* (2007), to detect spatio-temporal flood distributions in Cambodia and Vietnam. Sakamoto *et al.* (2005, 2006) derived a methodology to classify cropping systems (e.g., double-cropping system in the rainy/dry season, triple-cropping system) and noted regions where the number of crops per year was increased from two to three over the interval of 2002–2003. The modified approach developed in this study is applied to the EVI and LSWI time series to produce the flood inundation maps. In addition, the analysis has been carried out to determine the spatial extents and temporal changes of flood inundation within Bangladesh during the floods in 2007 and 2004. The above indices are estimated for each and every pixel using their basic time-series reflectance data produced by MODIS. The maps are a mere assemblage of these pixel results.

Modified algorithm of flood inundation maps

The algorithm used by the Sakamoto *et al.* (2007) was modified in this study. A flow chart of the modified method is shown in Figure 3. The previous algorithms used by Sakamoto *et al.* (2007) were examined and some components were excluded from the algorithm used here. In the previous algorithm, a wavelet-based filter was used to smooth data by removing the noise component and interpolating for any missing information. As a result, this algorithm creates artificial data and was not used in this study. The production of inundation maps in this study used a decision tree to associate each pixel with one of the following categories: the flood, mixed, nonflood and water-related pixels. The decision tree is illustrated in Figure 3 and may be summarized as follows:

- The first step was to detect cloud cover pixels from the image. If blue reflectance (band 3 of MODIS) is equal to or > 0.2 (Thenkabail *et al.*, 2005; Xiao *et al.*, 2006), it is considered as a cloudy pixel. Using this formula, the data related to cloudy pixels were removed from the image.
- The next step was to estimate EVI, LSWI and the difference value of EVI and LSWI, DVEL for each of the land class cover types.
- In this study, the discrimination of water-related pixels and nonflood pixels was conducted in accordance with the pioneering method developed by Xiao *et al.* (2005, 2006). The EVI, LSWI and DVEL are used exclusively to discriminate between the flood, mixed, nonflood and water-related pixels. The changes in EVI, LSI and DVEL for different land-use types are shown for 2007 in Figure 4.
- If the EVI is > 0.3, it can be classified as a nonflood-related pixel.
- The EVI curve of 'Forest' land-use type, for example in the Sundarbans, exhibits a value more than 0.3 during the year, except during the flood season.

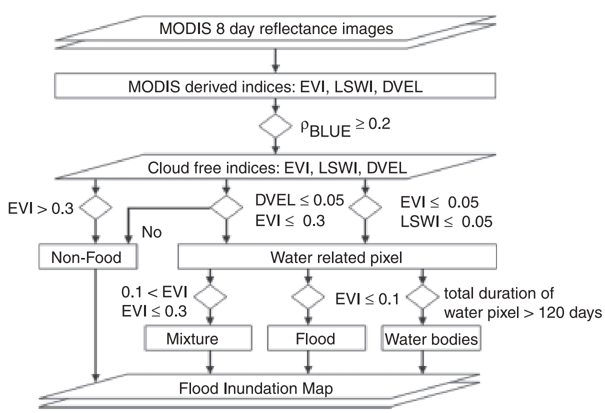

Figure 3 Flood chart for developing the flood inundation map using MODIS data.

© The Authors
Journal of Flood Risk Management © 2010 CIWEM and Blackwell Publishing Ltd

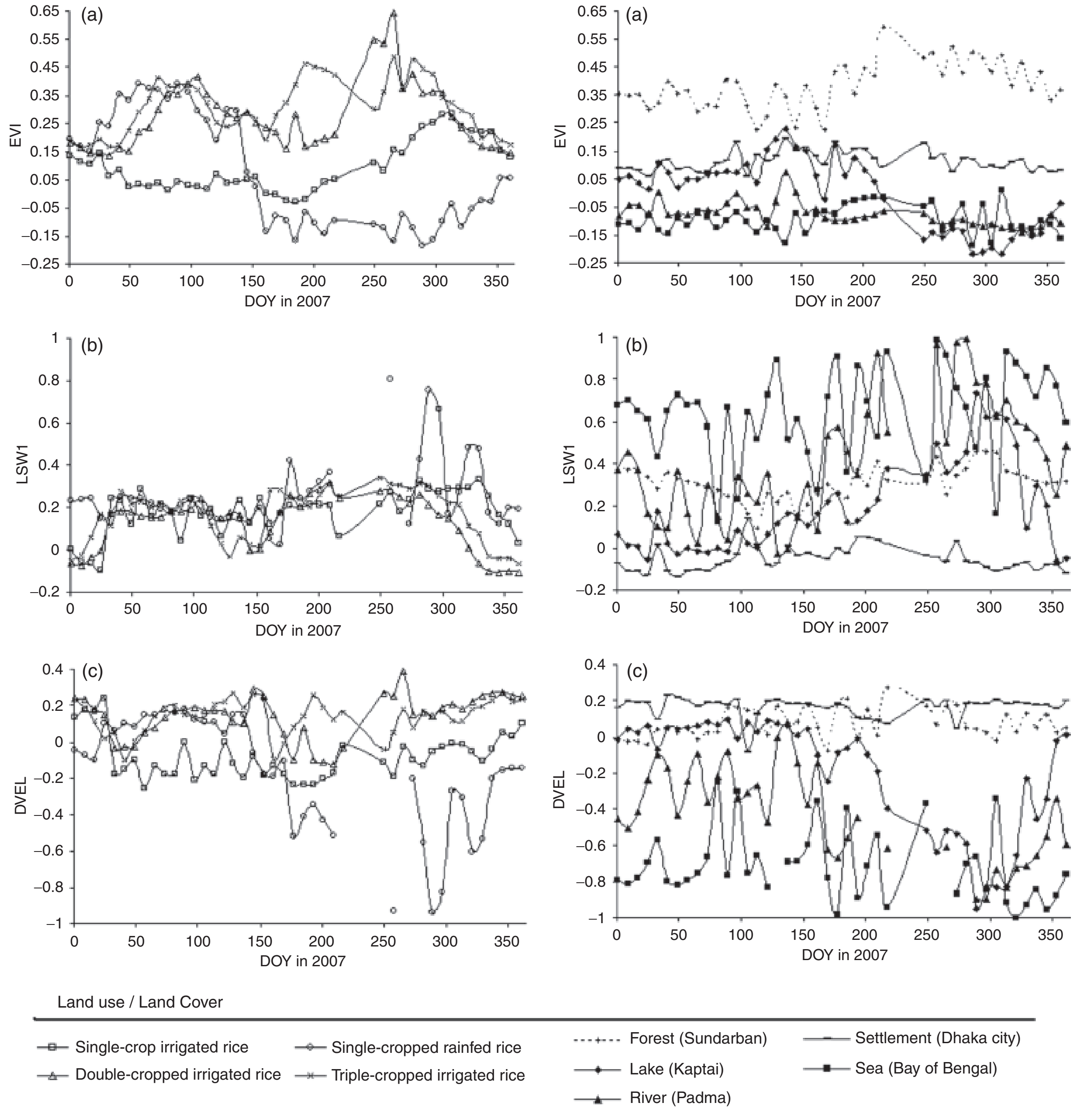

Figure 4 MODIS-derived indices: (a) EVI, (b) LSWI and (c) DVEL for the nine land use/land cover areas shown in Figure 1. LSWI, land surface water index.

- The EVI of permanent water bodies such as 'River' and 'Sea' land-use types are < 0.05 or even show negative values throughout the year.
- The DVEL of 'River' and 'Sea' land-use types have a DVEL value < 0.05. It can be inferred that water-related pixels should have a DVEL of < 0.05.
- However, excluding the 'Lake' land-use type, the DVEL value is not always < 0.05. To overcome this problem, another criterion is used to identify water-related pixels. In such cases, if the EVI is ≤ 0.05 and the LSWI is ≤ 0, the pixel will be identified as a water-related pixel.

After identifying the water-related pixels, it is essential to classify whether it is a flood pixel, a long-term water body or a mixed-type pixel. Because of the moderate-resolution (500 m) sensor of MODIS/TERRA, a pixel can be composed of a mixture of different types of land surfaces. It is difficult to discriminate between vegetation mixed with water and vegetation completely flooded by water. Figure 4 shows that the EVIs of 'Sea', 'Lake' or 'River' land types are below 0.1 and, as a

© The Authors
Journal of Flood Risk Management © 2010 CIWEM and Blackwell Publishing Ltd

result, this criterion can be used for a further classification of the water-related pixels. If a water-related pixel has an EVI of < 0.1, it will be considered as a flood pixel. If the EVI is > 0.1 but < 0.3, it will be identified as a mixed pixel. Finally, areas that are inundated throughout the year should be separated from the flood and mixed pixels. Many of the water bodies in Bangladesh have been identified as inundated, such as small wetlands known as 'Beels' and large wetlands known as 'Haors'. In these types of wetlands, water can be found for more than 6 months of the year. Therefore, the water-related pixels that have an inundation period of more than 120 days are classified as long-term water bodies.

This methodology was used to analyse changes in flood extent with time, and flood inundation maps were developed for 2004 and 2007.

Validation of proposed techniques

The modified technique used to identify the water surface from MODIS time-series data was validated through comparison with the standard product described below. Figure 5 shows four different types of images used to show similarities between the two outputs. Figure 5(a) shows the distributions of inundated regions on 28 July 2007 (DOY 209), which are determined using the MODIS images. In this figure, the flooded, mixed and long-term water bodies are represented by blue, green and white colours. The false-colour images of the MOD09 8-day composite data and the daily MOD09 data for the same date are shown in Figure 5(b). In the false-colour composite image, clouds are shown as white-coloured pixels. Long-term water bodies derived from MODIS data are also shown in the same Figure 5(c).

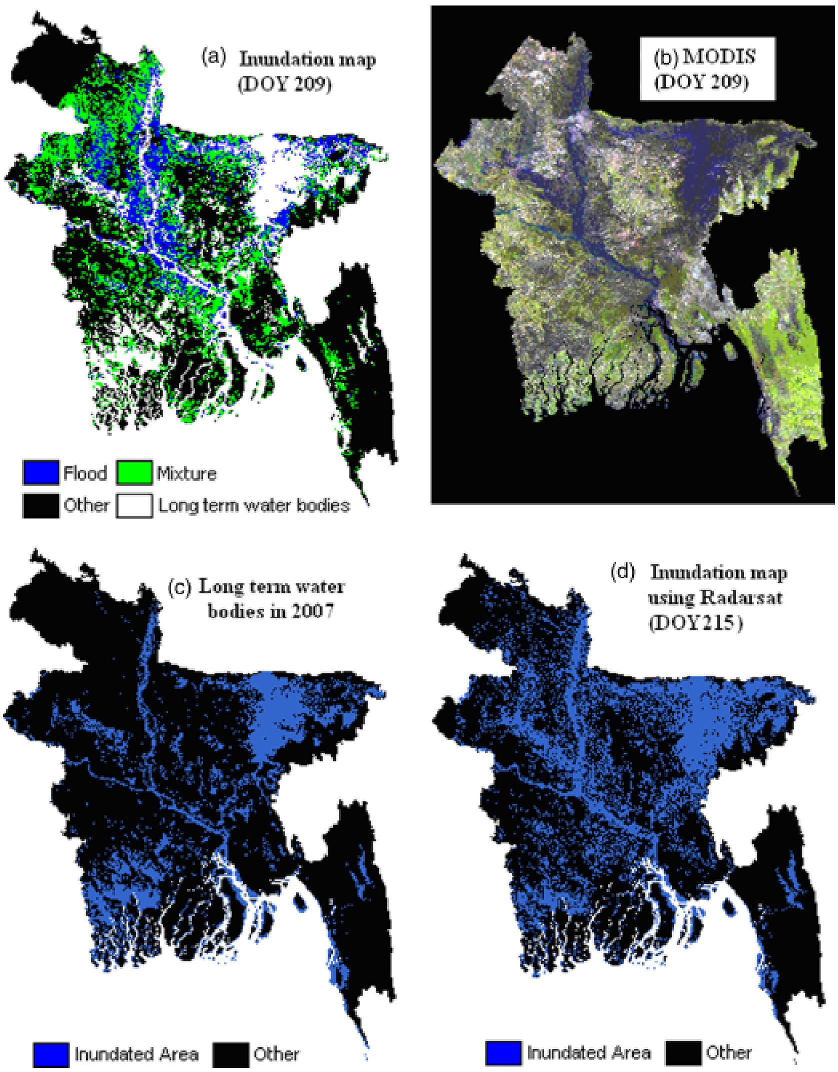

Figure 5 Spatial comparison of (a) MODIS-derived inundation map of 29 July 2007, (b) MODIS 8-day false-colour composite map (red is band 6, green is band 2 and blue is band 1) of 29 July 2007, (c) long-term water bodies in 2007 using MODIS data, (d) inundation map using the RADARSAT image on August 2003.

© The Authors
Journal of Flood Risk Management © 2010 CIWEM and Blackwell Publishing Ltd

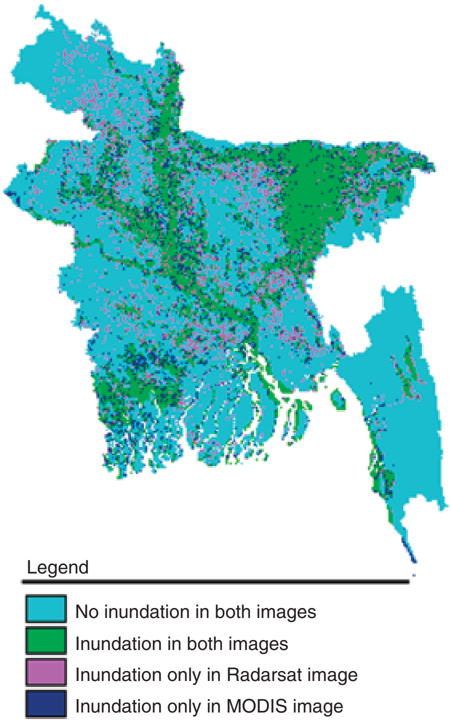

Figure 6 Overlay of the MODIS-derived inundation map on day osf the year (DOY) 209 with the nearest-available RADARSAT-derived inundation map on DOY 215. The inundation area derived from MODIS includes flood pixels and pixels of long-term water bodies.

The distribution of the inundation area on the 3 August of 2007 (DOY 215) using RADARSAT is shown in Figure 5(d). The inundation, shown in the RADARSAT images, was developed using a ruled-based method. A threshold value of more than 0.6 was considered as inundation in the area for the RADARSAT images. The inundated region is clearly identified in detail without any cloud-cover effects using RADARSAT images. The influence of cloud cover is considerably reduced in MOD09 8-day composite data as shown in Figure 5(b), although MOD09 production is not cloud free and needs correction for the removal of the clouds.

Figure 6 shows a comparison of the MODIS-derived inundation map for 28 July (DOY 209) with the closest available RADARSAT-derived inundation map for 3 August (DOY 215) using image crossing. Most of the areas in both images show quite a good match in the land-use patterns identified using these two types of satellite and sensors. However, there are differences: in the southern area, the MODIS shows a greater inundation area than RADARSAT; in the northeastern region, the RADARSAT image identifies a greater area as inundated than the MODIS image. Figure 7 shows the scattered plot produced from crossing both of the inundation maps. A comparison of the inundation areas derived from MODIS and RADARSAT produced an R^2 value of 0.96. The close agreement between these two

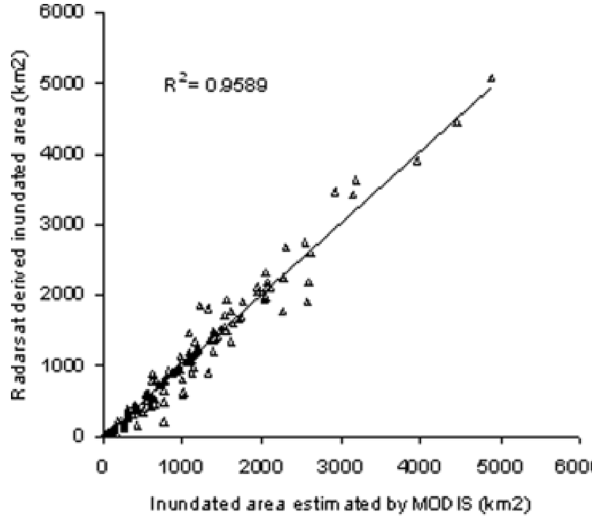

Figure 7 Correlation of the inundation area determined from MODIS with that of RADARSAT. The correlation coefficient R^2 is 0.96.

products provides a validation of the use of MODIS data and a modified algorithm for estimating inundated areas.

Although the inundation areas in both images have shown a high correlation, it is difficult to detect inundation in areas of high-vegetation coverage using moderate-resolution optical sensors such as MODIS. As a result, it is difficult to accurately identify the inundated area of flooded forests or marshes using the MODIS products. Figure 8 shows the temporal changes in flood and mixed land cover pixels for four types of paddy fields (single-cropped irrigated rice, single-cropped rain fed rice, double-cropped irrigated rice and triple-cropped irrigated rice), forest and settlement areas. During the flood season (May to September), more mixed pixels were found in the triple- and double-cropped irrigated areas than other land-use types. The mixed pixels may lead to an underestimation of flood extent when using MODIS outputs instead of the RADARSAT products. As a result, the northeastern region, where mostly double- and triple-irrigated rice grows, shows less flood pixels than in other regions. It is possible to enhance the estimation accuracy using DEM data or higher resolution data (Brivio *et al.*, 2002; Wang *et al.*, 2002); this approach, or a similar one, may warrant further investigation in the future. Although there is a fundamental overestimation problem resulting from mixed pixel effects, it is believed that temporal MODIS products still provide useful criteria for determining flood inundation.

Results and discussions

Spatial extents of floods in Bangladesh

The spatial extent of changes in flood inundation with the progress of floods can be visualized and assessed by

© The Authors
Journal of Flood Risk Management © 2010 CIWEM and Blackwell Publishing Ltd

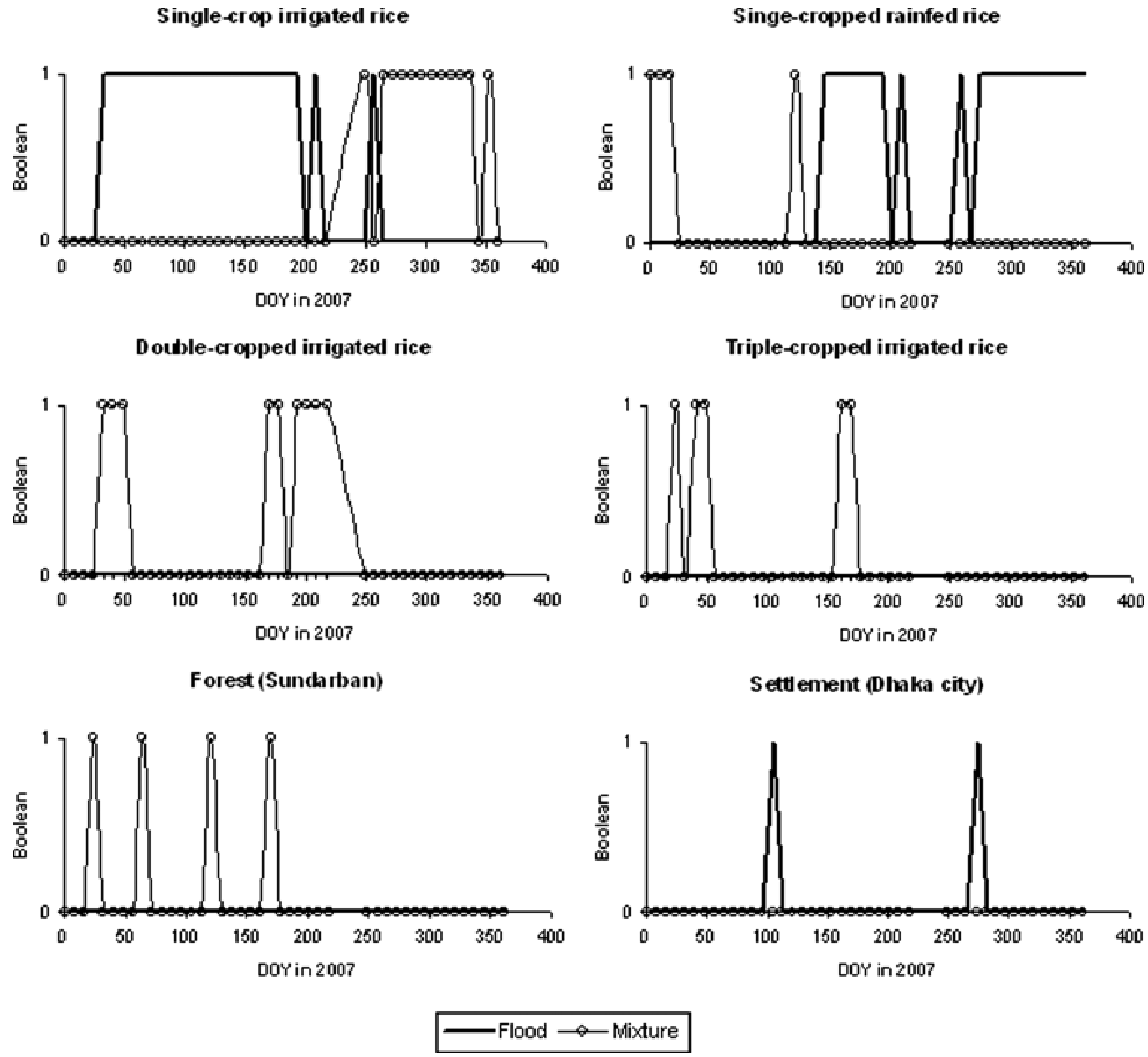

Figure 8 Temporal changes of flood and mixture pixels for four types of paddy fields (single-cropped irrigated rice, single-cropped rain fed rice, double-cropped irrigated rice and triple-cropped irrigated rice), forest and settlement areas.

displaying successive maps. This has been done for the 2007 and 2004 floods in Bangladesh. In Figure 9, the estimated flood area is shown from 20 July (DOY 201) to 5 August (DOY 217), during the floods in 2007 and 2004, respectively. In 2004, the flood started following a rapid increase in the water level from 20 July (Figure 2) and it reached its largest extent on 28 July (DOY 209). The flood of 2007 started 2 weeks later than the floods in 2004. In 2007, the water levels and the resulting inundation increased from 28 July (DOY 209) and the flood reached its largest extent on 5 August (DOY 217). The images also show how much the spatio-temporal distribution of the inundated area varies from year to year.

It is also possible to detect the maximum extent of the flooded area by overlaying a series of images during the flood (Sheng and Gong, 2001). This inundation map can be useful to create flood vulnerability maps and flood risk zones. In Figure 10, the maximum area of flood inundation is shown during the floods in 2004 and 2007, respectively. The blue, green and white colours represent areas of flood, mixture and long-term water bodies, respectively. Again, it is evident from this map that the extent of flooding varies from year to year. The areas that are common for both major floods should be classified as the most vulnerable areas. This information on the vulnerability of floods could potentially be useful for many purposes, e.g.

© The Authors
Journal of Flood Risk Management © 2010 CIWEM and Blackwell Publishing Ltd

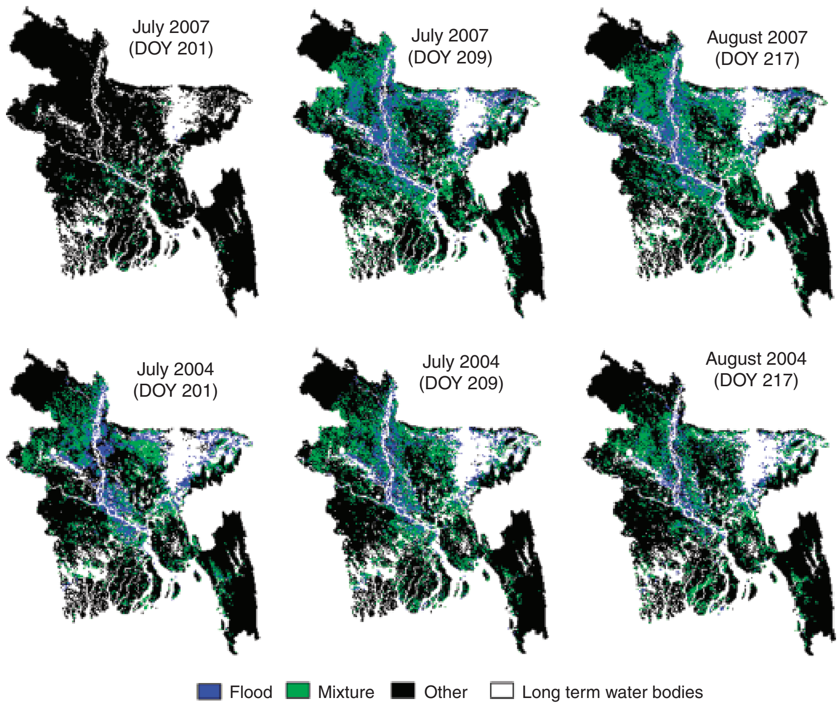

Figure 9 Spatial distribution of the flood-inundated area during the months of July and August of 2007 and 2004. Flood pixels are in blue colour. Mixture pixels are in green colour. Long-term water bodies are in white colour.

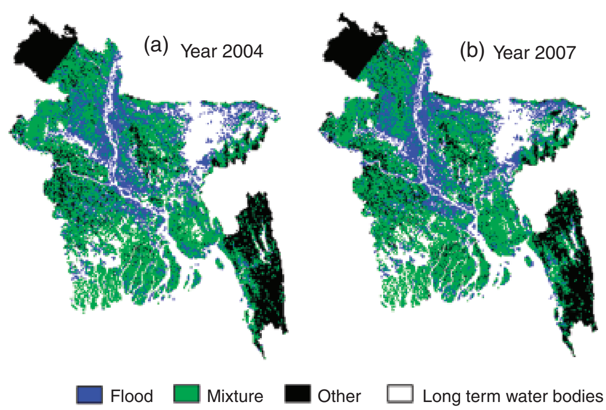

Figure 10 Flood inundation map of Bangladesh using MODIS images for (a) the Year 2004 and (b) the Year 2007. Flood pixels are in blue colour. Mixture pixels are in green colour. Long-term water bodies are in in white colour.

flood insurance, preparation of crop calendars and disaster management.

Temporal characteristics of floods

The start date, end date and duration of each flood can vary. The level of cloud cover in the wet season means that it is not possible to obtain cloud-free images every day. However, 8-day composite products can provide an image that is almost free from cloud and is atmospherically corrected. A time series of MODIS data could be used to determine these dates to the nearest week and to map the spatial extent of the flood. Figure 11 shows the estimates of the start dates, end dates and duration of inundation during the floods in 2007 and 2004. As these dates are based on images of the 8-day average value; it is not possible to represent the exact start and end day. However, these images can identify the starting and ending 'weeks' of the flood. Gauging stations can provide information about the date of crossing of the DL for a particular location on the river and the MODIS images can estimate the approximate date of crossing of the DL for each location of the riverbanks. This information could be helpful for farmers, fishermen and flood-preparedness activists.

The start dates for floods in 2004 are earlier than the start dates of the flood in 2007. The date of crossing the DL at Bahdurabad on the Brahmaputra River was 27 of July in 2007 and 11 July during the flood of 2004 (Figure 2). A similar pattern was found in the spatial distribution of the flooding identified in the maps for 2007 and 2004 (Figure 11). The duration of the floods at the Bahadurabad in the Brahmaputra River was found to be 21 days and 15 days during the floods in 2007 and 2004, respectively. The pixel information of the flood duration maps (Figure 11) shows more reddish colour for the floods in 2004 than for the floods in 2007.

© The Authors
Journal of Flood Risk Management © 2010 CIWEM and Blackwell Publishing Ltd

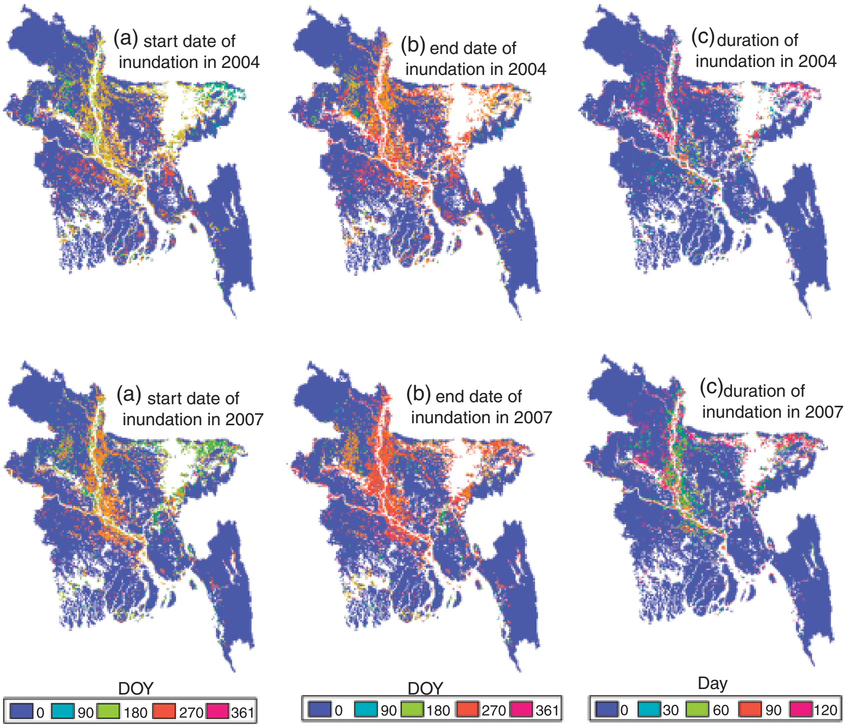

Figure 11 Spatial distribution of (a) start date, (b) end date and (c) duration of flood for 2004 and 2007.

At the Bhiarab Bazaar station on the Meghna River, the date of crossing the DL was 30 July and 11 July during the floods in 2007 and 2004, respectively (Figure 4.2). The flood pixels in Figure 4.11 show that the timing of the occurrence of flood pixels in 2004 and 2007 clearly has similar characteristics. The duration of floods above the DL at the Bhairab Bazaar station in the Meghna River in 2007 was 37 days and 38 days in the flood of 2004 (Figure 2). In the flood duration map, similar features were found for this river basin. The colour of inundation pixels is more reddish for floods in 2004 than that of 2007.

Conclusions

This study modifies a methodology developed by Sakamoto and colleagues to detect the spatial extents of, and temporal changes in, of flood inundation in Bangladesh during the monsoon season. Using this modified methodology, MODIS satellite images were used to develop flood inundation maps for the floods in 2007 and 2004. These low-resolution (500 m) MODIS-based area maps were compared with subsequent flood inundation maps based on the high-resolution (50 m) RADARSAT satellite images. The MODIS estimates show the strong correlation with the inundation areas derived from RADARSAT, with R^2 values of 0.96. This demonstrates that the flood maps derived from MODIS images can be used to characterize the floods. The inundation maps derived as a result of this research study will be useful for the integration of water resources and flood management and the maintenance of ecosystems of the wetlands of the People's Republic of Bangladesh.

Acknowledgements

The authors wish to express their sincere thanks to the Committee for Coordination and Development of the Institute of Water and Flood Management (IWFM), of Bangladesh University of Engineering and Technology (BUET), for taking initiatives to conduct this present study. Also, we wish to sincerely thank Prof. Rezaur Rahman, then director of the institute, for his continuous support for the successful completion of the research study.

References

Anderson E., Brakenridge G.R. & Caquard S. *Dartmouth Atlas of Global Flood Hazard: E100N20*. Hanover, USA: Dartmouth Flood Observatory, 2005. Available at http://www.dartmouth.edu/~floods/hydrography/E100N20.html (accessed 17 June 2010).

Asada H., Matsumuto J. & Rahman R. Impact of recent severe floods on rice production in Bangladesh. *Geogr Rev Jpn* 2005, **78**, (12), 783–793.

Brivio P.A., Colombo R., Maggi M. & Tomasoni R. Integration of remote sensing data and GIS for accurate mapping of flooded areas. *Int J Remote Sens* 2002, **23**, 429–441.

© The Authors
Journal of Flood Risk Management © 2010 CIWEM and Blackwell Publishing Ltd

Bryant R.G. & Rainey M.P. Investigation of flood inundation on playas within the Zone of Chotts, using a time-series of AVHRR. *Remote Sens Environ* 2002, **82**, 360–375.

Chowdhury J.U., Rahman R., Bala S.K. & Islam A.S. *Impact of 1998 flood on Dhaka city and performance of flood control works*. Dhaka: Institute of Flood Control & Drainage Research, Bangladesh University of Engineering & Technology, 1998.

Dartmouth Flood Observatory. *Dartmouth atlas of global flood hazard*. Hanover, New Hampshire, US: Dartmouth Flood Observatory, 2006. Available at http://www.dartmouth.edu/~floods/index.html (accessed 17 June 2010).

EOS. *NASA earth observing system data gateway*. Dhaka, Bangladesh: EOS, 2006. Available at http://eospso.gsfc.nasa.gov/eos_homepage/data_services.php (accessed 17 June 2010).

Gao B.C. DWI-A normalized difference water index for remote sensing of vegetation liquid water from space. *Remote Sens Environ* 1996, **58**, 257–266.

Harris A.R. & Mason I.M. Lake area measurement using AVHRR. *Int J Remote Sens* 1989, **10**, 885–895.

Henry J.B., Chastanet P., Fellah K. & Desons Y.L. ENVISAT multipolarised ASAR data for flood mapping. Paper presented at the IGRASS'03, Toulouse, France, 2003.

Heremans R., Willekens A., Borghys D., Verbeeck B., Valckenborgh J. & Acheroy M. Automatic detection of flooded areas on ENVISAT/ASAR images using an objected-oriented classification technique and active contour algorithm. Paper presented at the 31st International Symposium on Remote Sensing of the Environment, St. Petersburg, Russia, 2005.

Hirose K., Maruyama Y., Quy D.V., Tsukada M. & Shiokawa Y. Visualization of flood monitoring in the lower reaches of the Mekong River. Paper presented at the 22nd Asian Conference on Remote Sensing, Singapore, 2001.

Hossain A., Easson G., Justice V.J. & Mita D. Mapping flood extent, flood dynamics, and crop damage assessment using Radar Imagery Analysis. Mid-South Annual Engineering & Sciences Conference (MAESC), Oxford Conference Center, Oxford, MS, 17–18 May 2007.

Ishitsuka N., Saito G., Murakami T., Ogawa S. & Okamoto K. Methodology development for area determination of rice planted paddy using RADARSAT data. *J Remote Sens Soc Jpn* 2003, **23**, 458–472.

Islam A.S. & Chowdhury J.U., eds. *Hydrological characteristics of the 1998 flood in major rivers, engineering concern of flood*. Dhaka: Bangladesh University of Engineering and Technology, 2002.

Islam K.M.N. *Impacts of flood in urban Bangladesh: micro and macro level analysis*. A H Development Publishing House, Community Development Library, 2006.

Jackson T.J., Chen D., Cosh M., Li F., Anderson M. & Walthall C. Vegetation water content mapping using Landsat data derived normalized difference water index for corn and soybeans. *Remote Sens Environ* 2004, **92**, 475–482.

Jin Y.Q. A flooding index and its regional threshold value for monitoring floods in China from SSM/I data. *Int J Remote Sens* 1999, **20**, 1025–1030.

Laugier O., Fellah K., Tholey N., Meyer C. & De Fraipont P. High temporal detection and monitoring of flood zone dynamic using ERS data around catastrophic natural events: The 1993 and 1994 Camargue Flood events. Paper presented at the Proceedings of the third ERS Symposium, ESA SP-414, 1997.

Liew S.C., Chen P., Kam S.P., Tuong T.P., Minh V.Q. & Lim H. Rice crops monitoring in the Mekong River Delta using combined ERS and RADARSAT synthetic aperture radar. Paper presented at the IEEE International Geoscience and Remote Sensing Symposium (IGARSS'98), Seattle, USA, 1998.

Liu Z., Huang F., Li L. & Wan E. Dynamic monitoring and damage evaluation of flood in north-west Jilin with remote sensing. *Int J Remote Sens* 2002, **23**, 3669–3679.

Martineza J.M. & Toanb T. Mapping of flood dynamics and spatial distribution of vegetation in the Amazon floodplain using multitemporal SAR data. *Remote Sens Environ* 2007, **108**, (3), 209–223.

McFeeters S.K. The use of the Normalized Difference Water Index (NDWI) in the delineation of open water features. *Int J Remote Sens* 1996, **17**, 1425–1432.

Nguyen T.L. & Bui D.T. Flood monitoring of Mekong River delta, Vietnam using ERS SAR data. Paper presented at the 22nd Asian Conference on Remote Sensing, Singapore, 2001.

Rahman R., Haque A., Khan S.A., Salehin M. & Bala S.K. *Investigation of hydrologic aspects of flood-2004 with special emphasis on Dhaka city*. Dhaka, Bangladesh: Institute of Water and Flood Management (IWFM), Bangladesh University of Engineering and Technology (BUET), 2005.

Rogers A.S. & Kearney M.S. Reducing signature variability in unmixing coastal marsh Thematic Mapper scenes using spectral indices. *Int J Remote Sens* 2004, **20**, 2317–2335.

Sahoo R.N., Sehgal V.K., Kalra N. & Gupta R.K. Impact of flood dynamics on eastern Gangetic Agroecosystem: A remote sensing analysis, GIS Development. 2006. Available at http://www.gisdevelopment.net/proceedings/mapindia/2006/agriculture/mi06agri_195abs.htm (accessed 17 June 2010).

Sakamoto T., Nguyen N.V., Kotera A., Ohno H., Ishitsuka N. & Yokozawa M. Detecting temporal changes in the extent of annual flooding within the Cambodia and the Vietnamese Mekong Delta from MODIS time-series imagery. *Remote Sens Environ* 2007, **109**, (3), 295–313.

Sakamoto T., Nguyen N.V., Ohno H., Ishitsuka N. & Yokozawa M. Spatio-temporal distribution of rice phenology and cropping systems in the Mekong Delta with special reference to the seasonal water flow of the Mekong and Bassac rivers. *Remote Sens Environ* 2006, **100**, 1–16.

Sakamoto T., Yokozawa M., Toritani H., Shibayama M., Ishitsuka N. & Ohno H. A crop phenology detection method using time-series MODIS data. *Remote Sens Environ* 2005, **96**, 366–374.

Sheng Y. & Gong P. Quantitative dynamic flood monitoring with NOAA AVHRR. *Int J Remote Sens* 2001, **22**, 1709–1724.

Tanaka M., Sugimura T. & Tanaka S. Monitoring water surface ratio in the Chinese floods of summer 1998 by DMSP-SMM/I. *Int J Remote Sens* 2000, **21**, 1561–1569.

© The Authors
Journal of Flood Risk Management © 2010 CIWEM and Blackwell Publishing Ltd

Tanaka M., Sugimura T., Tanaka S. & Tamai N. Flood-drought cycle of Tonle Sap and Mekong Delta area observed by DMSP-SSM/I. *Int J Remote Sens* 2003, **24**, 1487–1504.

TBRS. Theoretical basis for the enhanced vegetation index.2002. Available at http://tbrs.arizona.edu/cdrom/VI_Intro/EVI_Theo.html (accessed 17 June 2010).

Thenkabail P.S., Schull M. & Turral H. Ganges and Indus river basin land use/land cover (LULC) and irrigated area mapping using continuous streams of MODIS data. *Remote Sens Environ* 2005, **95**, 317–341.

Tong P.H.S., Auda Y., Populus J., Aizpuru M., Habshi A.A. & Blasco F. Assessment from space of mangroves evolution in the Mekong Delta, in relation to extensive shrimp farming. *Int J Remote Sens* 2004, **25**, 4795–4812.

Vermote E.F. & Vermeulen A.MODIS algorithm technical background document, atmospheric correction algorithm: spectral reflectances (MOD09). NASA contract NAS5-96062, 1999.

Wang Y. Mapping the extent of a flood: what we have learned and how we could do better. *Nat Hazard Rev* 2002, **3**, 68–73.

Wang Y. Seasonal change in the extent of inundation on floodplains detected by JERS-1 Synthetic Aperture Radar data. *Int J Remote Sens* 2004, **25**, 2497–2508.

Wang Y., Colby J.D. & Mulcahy K.A. An efficient method for mapping flood extent in a coastal floodplain using Landsat TM and DEM data. *Int J Remote Sens* 2002, **23**, 3681–3691.

Xiao X., Boles S., Frolking S., Li C., Bau J.Y. & Salas W. Mapping paddy rice agriculture in South and Southeast Asia using multitemporal MODIS images. *Remote Sens Environ* 2006, **100**, 95–113.

Xiao X., Boles S., Frolking S., Salas W., Moore III B. & Li C. Landscape-scale characterization of cropland in China using vegetation and Landsat TM images. *Int J Remote Sens* 2002a, **23**, 3579–3594.

Xiao X., Boles S., Frolking S., Salas W., Moore III B. & Li C. Observation of flooding and rice transplanting of paddy rice fields at the site to landscape scales in China using VEGETATION sensor data. *Int J Remote Sens* 2002b, **23**, 3009–3022.

Xiao X., Boles S., Liu J., Zuang D., Frolking S. & Li C. Mapping paddy rice agriculture in southern China using multi-temporal MODIS images. *Remote Sens Environ* 2005, **95**, 480–492.

Zhan X., Sohlberg R.A., Townshend J.R.G., DiMiceli C., Carroll M.L. & Eastman J.C. Detection of land cover change using MODIS 250 m data. *Remote Sens Environ* 2002, **83**, 336–350.

© The Authors
Journal of Flood Risk Management © 2010 CIWEM and Blackwell Publishing Ltd

View publication stats